Electronic properties of perfect and nonperfect one-dimensional quasicrystals

Youyan Liu* and Rolf Riklund
Department of Physics and Measurement Technology, University of Linköping, S-581 83 Linköping, Sweden
(Received 12 November 1986)

We study the on-site model of a one-dimensional Fibonacci lattice. It is found that, compared with the transfer model, the electronic spectrum has different global structure, but the same branching rule in the following hierarchies. The relationship between the numbers of constructing elements of the lattice and the numbers of eigenstates in subbands is established. The improved Dean method for solving eigenenergies and eigenfunctions and the transfer-matrix method are used to examine the localization in very large samples. Three kinds of wave-function behavior (extended, localized, and intermediate states) are definitely found. The effect of fluctuation in the site energies, which simulates the randomness of layer thickness in experimental samples grown by molecular-beam epitaxy, is numerically examined. Following the increase of fluctuation up to ±40%, the band structure changes very little. But even very small fluctuations will dramatically change the extended states to localized states, which agrees with the theory of one-dimensional disordered systems.

Following the important experimental discovery of the icosahedral symmetry in the metallic alloy Al-Mn by Shechtman *et al.*,[1] a new research field of condensed state physics has been opened. Levine and Steinhardt[2] proposed a three-dimensional Penrose tiling as the basic structure to explain how icosahedral symmetry can coexist with long-range order. At the same time, Merlin *et al.*[3] have successively grown a quasiperiodic Fibonacci superlattice and carried out x-ray and Raman scattering measurements. These experiments have stimulated the interest in the study of one-dimensional quasiperiodic systems.

The Fibonacci lattice is the one-dimensional analog of the Penrose tiling and the icosahedral quasicrystal.[4–7] This analog can be determined by the projecting technique, which systematically constructs the quasicrystalline structure in various spatial dimensions in a unified way. In the Fibonacci lattice there are two kinds of models based on the tight-binding Hamiltonian,

$$H=\sum_{n=-\infty}^{\infty} E(n)\,|\,n\rangle\langle n\,|+\sum_{n=-\infty}^{\infty}[t_{n,n+1}\,|\,n\rangle\langle n+1\,|+t_{n,n-1}\,|\,n\rangle\langle n-1\,|\,], \tag{1}$$

where $E(n)$ is the single-site energy and $t_{n,n\pm1}$ is the nearest-neighbor hopping integral. For the on-site model, the site energies consist of E_A and $E_B=-E_A$, which are given by the Fibonacci sequence. The other model is the transfer model, the Hamiltonian of which has a constant-site energy, but contains two kinds of hopping integrals t_A and t_B, which are arranged according to the Fibonacci sequence.

Recently, the transfer model has been extensively studied.[8–14] However, very little has been published for the on-site model. Using renormalization-group methods, Kohmoto *et al.*[15] and Ostlund *et al.*[16] treat the on-site model and get some results on the properties of spectrum and wave functions. In this paper, we concentrate on the on-site model of the Fibonacci sequence. In Sec. I, we investigate the energy spectrum, which is found to be quite different from the transfer model in the global structure of the electron spectrum, but not in the phonon spectrum. In Sec. II, the localization of the electronic wave function is examined by different approaches. The three kinds of wave-function behavior, extended state, localized state, and intermediate state, are definitely found. Finally, in Sec. III we numerically investigate the effect of fluctuation in the site energy, which corresponds to the fluctuation of the layer thickness in the experimental samples.[17] It has been found that the influence on the band structure is very small for modest fluctuations, but that the breaking of the quasicrystalline order results in the localization of all eigenstates.

I. ELECTRONIC AND VIBRATIONAL SPECTRUM OF THE FIBONACCI CHAIN

For simplicity, we consider the studied one-dimensional model of the lattice as a chain of atoms, which contains two different kinds of atoms, A and B. The Fibonacci chain is defined by the generating rule $A\rightarrow AB$ and $B\rightarrow A$, starting with B. Let F_n be the number of atoms in the nth generation, then the set (F_n) satisfies the recursion relation

$$F_i=F_{i-1}+F_{i-2}\ . \tag{2}$$

The chain, such as $ABAABABAABAAB$ for the seventh generation, can also be considered to be built up of three kinds of constructing elements, A, AA, and B. Let N_A^i, N_{AA}^i, and N_B^i be the numbers of the constructing elements, respectively. For the ith generation sequence, by the induction method we have found the following distribution rule:

$$N_B^i=F_{i-2},\quad N_A^i=F_{i-4},\quad N_{AA}^i=F_{i-3}\ ,\quad \text{odd } i\ ,$$

$$N_B^i=F_{i-2},\quad N_A^i=F_{i-4}+2,\quad N_{AA}^i=F_{i-3}-1\ ,\quad \text{even } i\ .$$

This distribution is very important for the electronic spectrum. From the distribution rule above, we can easily calculate the ratio of the number of the two different kinds of atoms,

$$r=\frac{N_B}{N_A}=\lim_{i\to\infty}\frac{F_{i-2}}{F_{i-2}+F_{i-3}}=\lim_{i\to\infty}\cfrac{1}{1+\cfrac{1}{1+\ddots+\cfrac{F_{n-1}}{F_n}}}=1/\tau$$

where τ is the golden mean.

For the on-site model of the Fibonacci chain, the equation of motion for the amplitudes of the electronic eigenfunction $\Psi=\sum_n a_n \mid n\rangle$ is

$$[\varepsilon-E(n)]a_n-a_{n+1}-a_{n-1}=0\ , \tag{3}$$

where we have taken the nearest-neighbor hopping integral $t=-1$. Using a direct diagonalization method with a rigid boundary condition, we obtain the electronic spectrum for the 13th generation Fibonacci sequence. In Fig. 1, where we choose the site energy $E_A=\mid E_B\mid=1$, the 233 eigenenergies are shown as a function of the order of their magnitude. A four-subband global structure can be clearly seen, which is different from the three-subband global structure in the transfer model. But in each of the following hierarchies, these two models have the same branching rule. Each subband, according to the $F_i=F_{i-2}+F_{i-3}+F_{i-2}$ rule, is divided into three subsubbands until it is unresolvable. This four-subband global structure is characteristic of the electronic spectrum of the on-site model. In Fig. 2, where the physical parameters are the same as in Fig. 1, we schematically show how the four-subband structure is formed. First, all the levels of the electrons derived from atoms B form the lowest subband, which we call the B subband. This is because atom B always has atom A and cluster AA as its neighbors, so its energy eigenstate is pushed to a level which is lower than its "bare" energy, i.e., the site energy $E_B=-1$. This point is well known for disordered systems. In the same way, all the isolated atoms A generate the A subband, which is the second upper subband in Fig. 2. However, the two bare levels of the AA cluster split and form two AA subbands. The width of splitting depends on the difference between E_A and E_B, if we keep the hopping integral t unchanged (see Fig. 3).

Now we know the numbers of the eigenstates in each subband. We rewrite F_i as

$$F_i=F_{i-2}+F_{i-3}+F_{i-4}+F_{i-3}\ .$$

If i is an odd number, the number of eigenstates is F_{i-2} in the B subband, F_{i-4} in the A subband, and F_{i-3} in each one of the two AA subbands, respectively. The above formula gives the distribution of the numbers of eigenstates in the four subbands. If i is an even number, then N^i_{AA}, the number of clusters AA, is $F_{i-3}-1$ and N^i_A is $F_{i-4}+2$. But in this case, the first and last atoms of the Fibonacci chain are A atoms. Correspondingly, there are two surface states in the two ends of the A subband, as is shown in Fig. 3. They can be considered to join two neighbor AA subbands. In this way, the structure of the case with i even is the same as the case with i odd. In fact, this argument can be easily understood if we connect two ends of the Fibonacci chain as a ring, then although i is even, the distribution rule, $N^i_B=F_{i-2}$, $N^i_{AA}=F_{i-3}$, $N^i_A=F_{i-4}$, holds exactly.

This four-subband structure no longer appears in the following hierarchy, but is instead replaced by a one- split to three-subband self-similar structure. The reason is that the Fibonacci lattice is constructed from three kinds of constructing elements A, B, and AA. They quasiperiodically alternate and in this way generate the one- split to three-subband self-similar structure.

Figure 3, where $i=12$ (generation) and $t=-1$, shows the site energy versus eigenenergy phase diagram, where

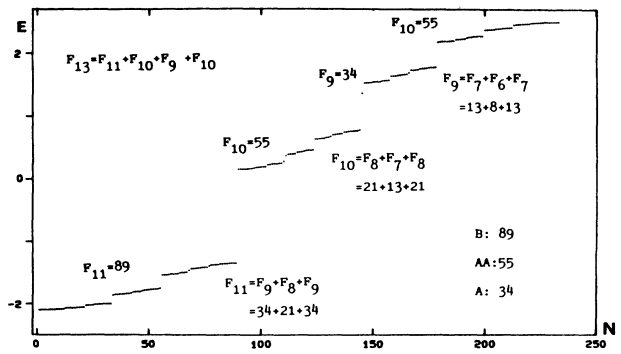

FIG. 1. Electronic spectrum for an on-site model of Fibonacci lattice with two site energies $E_A=-E_B=1$, for 13th generation. The N labels the eigenstate with energy E_N. The four-subband global structure, the one- split to three-subband hierarchical structure, the number of constructing elements, and the distribution rules are shown.

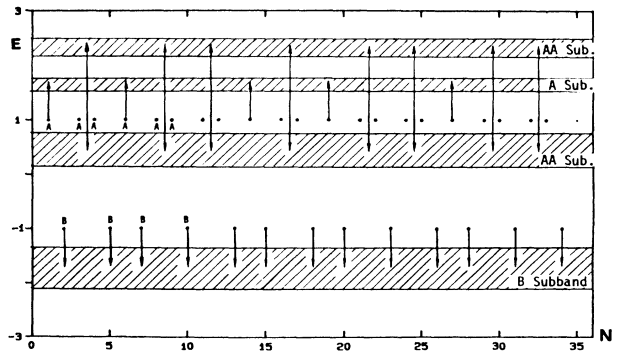

FIG. 2. Schematic picture illustrating the formation of the four main subbands from the constructing elements A, AA, and B. N are the coordinates of atoms in the Fibonacci chain. A and B form their subbands and AA forms two subbands, respectively. The "bare" site energies are $E_A=-E_B=1$, and the hopping integral $t=-1$.

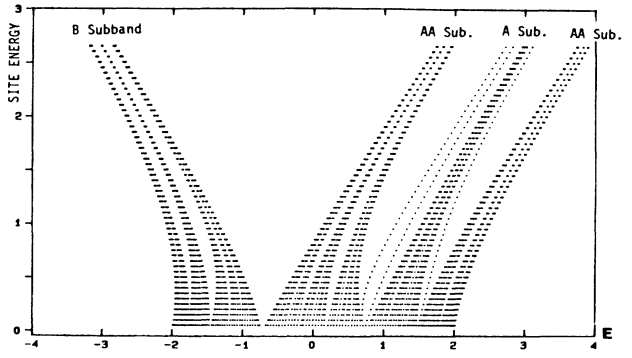

FIG. 3. Phase diagram in the site energy amplitude vs eigenenergy plane for the 12th generation Fibonacci chain with $E_A=-E_B=1$, $t=-1$. Four-subband global structure, hierarchical structure, and surface state are shown.

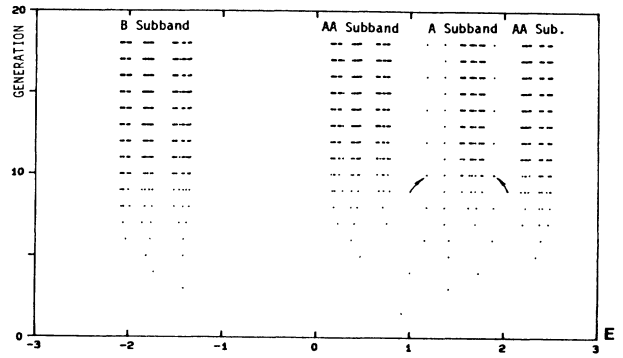

FIG. 4. Phase diagram in the generation versus eigenenergy plane for 12th generation Fibonacci chain with $E_A=-E_B=1$, $t=-1$. Arrows indicate the surface states appearing for even generation. The gross band structures become the same for even or odd number of generations above 12th generation (see text).

we can clearly see the four-main-subband global structure and the one- split to three-subband hierarchical structure in the following substructures. We also can see two surface states, which compensate two neighbor AA subbands to complete the self-similar hierarchical structure. It is interesting to see that when the site energy is small, these two surface states definitely locate in the AA subbands. With the increase of site energy they leave the AA subbands and come close to the A subband. In Fig. 4, we show the distributions of the electronic eigenenergy for different generation in the on-site model under the rigid boundary condition. We can see that above a certain generation the gross band structure does not change, irrespective of the system size. The position of the main bands and gaps remains unchanged with the increase of the Fibonacci generation. The eigenstates generated by increasing the number of generation only fill the band regions of the previous generation. This result is the same as in the transfer model[12] and is different from the random binary system. In Fig. 4, if the generation i is even, we can also see the two interesting surface states compensating two AA subbands. We notice that when compared with one of the odd-i generations, the AA subband of the even-i generation is a little bit shorter in the end closest to the A subband. This suggests that these two states belong to the AA subbands. We also should notice that above a certain generation, for the odd-i generations or for the even-i generations the gross band structure does not change. But both of them are different from each other, because these two cases have different surface states which would slightly change the positions and the widths of the subbands.

The four-main-subband global structure is a quantum-mechanical effect for electrons. We thus expect the global structure of the phonon spectrum to be different. For the on-site model of the harmonic Fibonacci chain, if we set the strength of the harmonic coupling equal to unity, then the equation of motion for the displacement u_i from its equilibrium position is

$$-m_i\omega^2 u_i = u_{i+1}+u_{i-1}-2u_i \ .$$

Here m_i is the mass of the ith atom, which is given by a Fibonacci sequence. Figure 5, where we set $m_A=2$ and $m_B=1$, shows the phonon spectrum for the 15th generation Fibonacci chain. This spectrum, as we expect, has a three-subband global structure and each subband, according to the $F_i=F_{i-2}+F_{i-3}+F_{i-2}$ rule, is divided into three sub-subbands and so on. This result is the same as for the transfer model.[10] This structure with three branches, in principle, contains one acoustical branch and two optical branches which correspond to two kinds of relative vibrations between A and A, or A and B. The self-similar structure again comes from the quasiperiodicity of the Fibonacci sequence.

II. LOCALIZATION

As an analog, it is worthwhile to recall some results for the Aubry model of one-dimensional incommensurate systems.[18] Avron and Simon have suggested that at the $V=2t$ critical point, where V is the strength of the incommensurate potential and t is the nearest-neighbor hopping integral, the spectrum is singular continuous and the

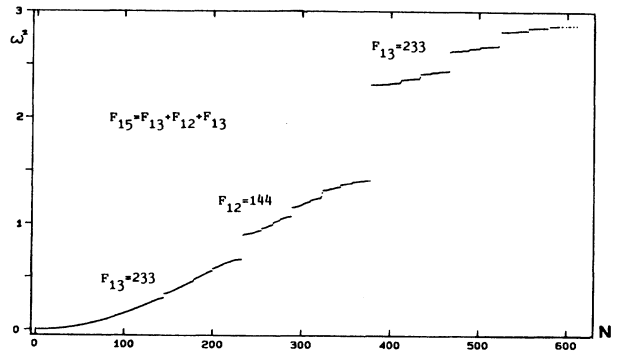

FIG. 5. Phonon spectrum for an on-site model of a Fibonacci lattice with masses of atoms $m_A=2$ and $m_B=1$ for 15th generation. The N is the mode number. The three-subband global structure and the self-similar structure are shown.

have unusual behavior, decaying practically to zero and then recovering to large values, for wave vector Q equal to an ordinary irrational number. In the works of Kohmoto *et al.*[15] and Ostlund *et al.*,[16] by choosing a specific discontinuous periodic potential whose period is incommensurate with the lattice period, they reduce the Schrödinger equation to a recursion relation for the transfer matrices which follow the Fibonacci sequence. Because the diagonal matrix elements of the transfer matrices are quasiperiodic, this corresponds to the on-site model of the Fibonacci sequence. They conclude that the spectral measure is singular continuous and the wave function is critical. Recently, Kohmoto[9] directly treated the Fibonacci sequence; the result is confirmed and there are two types of wave functions: self-similar and chaotic. Thouless and Niu,[19] using the scaling theory of wave function, under some approximation conclude that at critical point $V=2t$, the wave function has a power-law decay, which is energy dependent. On the other hand, using the successive average resistivity as the criterion of localization, one of the present authors[20] has numerically shown that at the critical point the localization of the wave function depends on the wave vector and eigenenergy, and that the extended states, localized states, and intermediate states coexist. Therefore, the wave-function behavior of a Fibonacci sequence is an interesting and open problem.

For examining the localization of the on-site model of the Fibonacci sequence, we firstly use the eigenvalue-Dy-Wu-Wongtawotnugool (EDWW) method[21] to calculate the eigenenergies, eigenvectors, first moment, second moment, and inverse participation ratio[22] (IPR) under a rigid boundary condition.

The ith normalized eigenfunction can be expressed as

$$|\Psi_i\rangle=\sum_{j=1}^{N} B_{ji}|j\rangle \ .$$

Then the corresponding IPR is defined as

$$I_i=\sum_{j=1}^{N}|B_{ji}|^4 \ .$$

If we take the atom spacing as the unit of length, then the first moment is defined as

$$M_i=\frac{1}{N}\sum_{j=1}^{N} jB_{ij}^2$$

and the second moment is defined as

$$S_i=\frac{1}{N}\left[\sum_{j=1}^{N} j^2|B_{ji}|^2-\left[\sum_{j=1}^{N} j|B_{ji}|^2\right]^2\right]^{1/2} \ .$$

The first moment gives the center of gravity of the wave function, the IPR and second moment, from a different aspect, measure the localization of the wave function. The IPR is a measure of the inverse of the number of sites occupied by the wave function and the second moment is a measure of the extension of the wave function.

Figure 6 shows the numerical results of the EDWW method for an 18th generation Fibonacci sequence ($N=2584$). In Fig. 6(a), we plot the first moment versus eigenenergy, where we can see the four-main-subband global structure and the one- split to three-subband hierarchical structure. At the same time, we can also see that the center of gravity of the eigenfunctions spread over the whole system, but the majority has the center of gravity in the middle region. In Fig. 6(b), we can see a large variation in the second moments, which suggests the coexistence of three kinds of wave functions: extended, localized, and intermediate (unusual wave-function behavior). The same conclusion can be drawn from Fig. 6(c), which shows the IPR versus eigenenergy and where also the self-similarity of the structure can be seen.

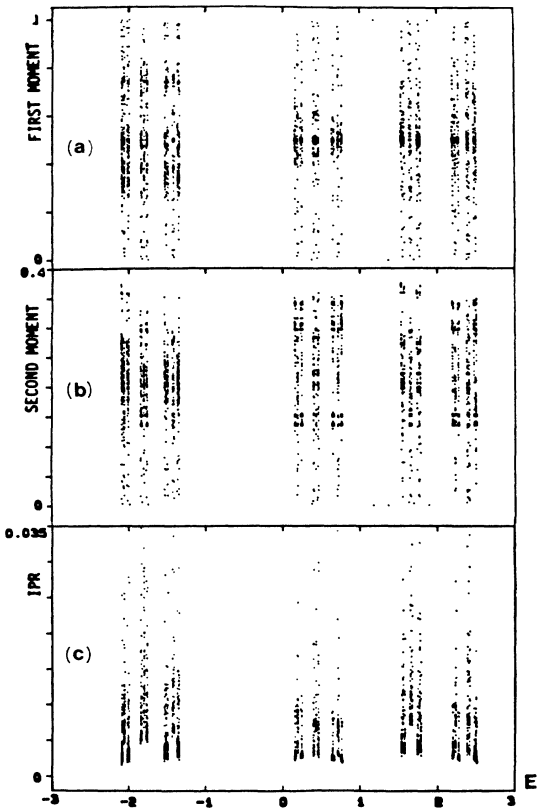

FIG. 6. The first moments, second moments, and the IPR versus eigenenergy for the 18th generation ($N=2584$) are shown by Figs. 6(a), 6(b), and 6(c), respectively. The site energies $E_A=-E_B=1$. Figure 6(a) shows that the center of gravity of the wave functions spreads over the whole chain, but that the middle part of it has bigger probability. Figures 6(b) and 6(c), which display the second moment and IPR respectively, show that the localizations of eigenstates are quite different from each other. The IPR spectrum also clearly exhibits the self-similarity.

More solid evidence of the coexistence of the different localization is the behavior of the wave functions themselves. We use the EDWW method again for a 21st generation Fibonacci sequence, which contains $N=10946$ atoms. In Fig. 7 we show the extended, intermediate, localized, and surface states, respectively, which also displays some kind of quasiperiodicity. But, it is evident

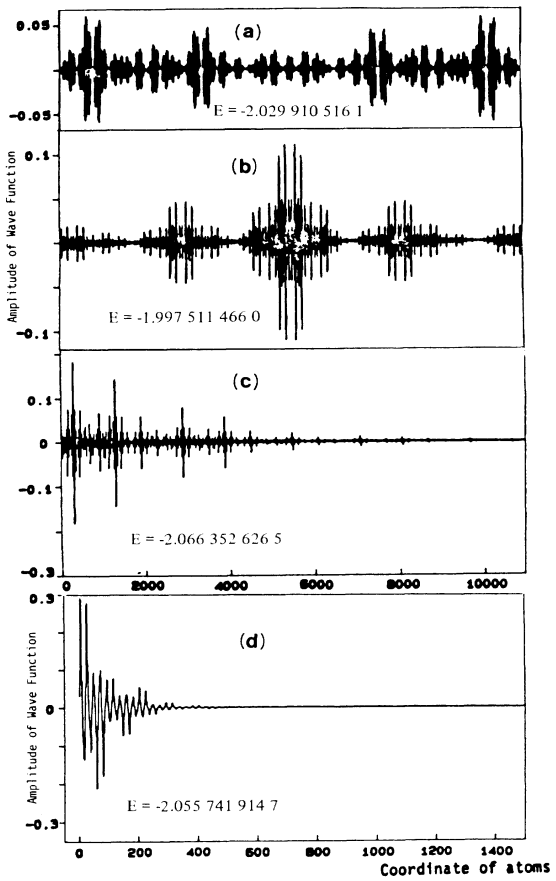

FIG. 7. Wave functions with different localizations for 21st generation Fibonacci chain ($N=10946$). Site energies $E_A=-E_B=1$, hopping integral $t=1$. (a) case is a wavelike extended state, (b) case is an intermediate state, and (c) case is a localized state with slow power-law decay. Fig. 7(d) shows a surface state. Note that in panel (d) only a fraction of the whole chain is plotted.

that different localizations of the eigenstates coexist for the Fibonacci quasicrystal.

To confirm the above conclusion, we have calculated the resistivity, which is a plausible physical quantity for estimating the localization and can be examined, in principle, by experiment. For calculating the resistivity, the Landauer formula combined with the transfer matrix method is very powerful and has been used by many authors in the disordered and one-dimensional incommensurate systems.[18,23,24]

We embed a segment of the Fibonacci lattice, which contains $N+1$ atoms and is of length N (here the lattice spacing is taken as unity) in an infinite, perfectly conducting, ordered chain. For this system the tight-binding Hamiltonian is

$$H=\sum_{n=-\infty}^{\infty} E(n)\,|\,n\rangle\langle n\,| + \sum_{n=-\infty}^{\infty} t(\,|\,n\rangle\langle n+1\,| + |\,n+1\rangle\langle n\,|\,),$$

where t is the hopping integral and $E(n)$ are the site energies. In the perfect ordered chain we take $E(n)$ to be zero, and in the Fibonacci segment, $E_A=-E_B=1$.

The equation of motion for the amplitudes of eigenfunction is

$$[\varepsilon-E(n)]a_n-a_{n+1}-a_{n-1}=0\ . \tag{3}$$

We define the promotion matrix as follows:

$$P^{(n)}\begin{bmatrix}a_n\\a_{n-1}\end{bmatrix}=\begin{bmatrix}\varepsilon-E(n) & -1\\ 1 & 0\end{bmatrix}\begin{bmatrix}a_n\\a_{n-1}\end{bmatrix}=\begin{bmatrix}a_{n+1}\\a_n\end{bmatrix}. \tag{4}$$

The relation which connects both ends of the Fibonacci segment is

$$\begin{bmatrix}a_{N+2}\\a_{N+1}\end{bmatrix}=\begin{bmatrix}\prod_{i=1}^{N+1} P^{(i)}\end{bmatrix}\begin{bmatrix}a_1\\a_0\end{bmatrix}=P_N\begin{bmatrix}a_1\\a_0\end{bmatrix}. \tag{5}$$

In the left and right perfect conductors of the Fibonacci segment the normalized eigenfunction can be written as

$$a_n=\begin{cases}Ae^{ikn}+Be^{-ikn}, & -\infty<n\le 1\ ,\\ Ce^{ikn}+De^{-ikn}, & N+1\le n<\infty\ .\end{cases} \tag{6}$$

We define the transfer matrix T_N by

$$T_N\begin{bmatrix}B\\A\end{bmatrix}=\begin{bmatrix}D\\C\end{bmatrix}. \tag{7}$$

Now we assume a situation, where a particle is incident to the Fibonacci segment from the left perfect-ordered chain. We take the incident amplitude to be unity. If the total reflection amplitude from the segment is r_N and the total transmission amplitude is t_N, then

$$a_n=\begin{cases}e^{ikt}+r_Ne^{-ikt}, & n=0,-1,-2,\ldots\\ t_Ne^{ikt}, & n\ge N+1\ .\end{cases} \tag{8}$$

From the definition of T_N, we have

$$\begin{bmatrix}0\\t_N\end{bmatrix}=T_N\begin{bmatrix}r_N\\1\end{bmatrix}=\begin{bmatrix}T_{N11} & T_{N12}\\ T_{N21} & T_{N22}\end{bmatrix}\begin{bmatrix}r_N\\1\end{bmatrix}, \tag{9}$$

$$r_N=-T_{N12}/T_{N11}\ ,\quad t_N=1/T_{N11}\ . \tag{10}$$

The reflection coefficient is

$$R_N=|\,r_N\,|^2=T_{N12}T^*_{N12}/T_{N11}T^*_{N11} \tag{11}$$

and the transmission coefficient is

$$T_N=|\,t_N\,|^2=1/(T_{N11}T^*_{N11})\ , \tag{12}$$

where T_{Nij} is the element of transfer matrix T_N. $T_N=\Theta S^{-1}P_NS$,

$$\Theta=\begin{bmatrix}e^{ik(N+1)} & 0\\ 0 & e^{-ik(N+1)}\end{bmatrix},\quad S=\begin{bmatrix}e^{-ik} & e^{ik}\\ 1 & 1\end{bmatrix}. \tag{13}$$

The Landauer formula for the energy-dependent dimensionless resistance $R(E)$ of a finite one-dimensional system embedded in a perfect-ordered chain is

$$R(E,N)=R_N/T_N=|\,T_{N12}\,|^2\ . \tag{14}$$

For finding an effective criterion of localization suitable for the transfer matrix method, we examine the average resistivity $\bar{\rho}$ which is defined as

$$\bar{\rho}_N = \sum_{i=1}^{N} \rho_i / N = (1/N)[R(E,1)/1 + R(E,2)/2 + \cdots + R(E,N)/N] , \tag{15}$$

where N is the length of the Fibonacci segment, $R(E,j)$ is the dimensionless resistance which is determined by the Landauer formula (14).

For the metallic crystalline solids, $\bar{\rho}$ should be independent of the size of the system, so at zero temperature $\bar{\rho}=\rho_i=\rho=0$.

For an extended state in the Fibonacci lattice, the reflection coefficient is smaller than unity, so we have

$$\rho_N = (R_N/1-R_N)(1/N) \overset{N\to\infty}{\longrightarrow} 0$$

and

$$\bar{\rho}_N \overset{N\to\infty}{\longrightarrow} 0 .$$

Therefore, if we successively calculate the respective average resistivities with increasing N, after reaching some value of N, the average resistivities will monotonously decrease if the state is extended. Quite to the contrary, if the state is localized, no matter how the resistance exponentially increases for the usual disordered case, i.e., $R(E,N) \propto e^{N/\xi}$, or by the power-law increases, as for some special weak localization case,[25] i.e., $R(E,N) \propto (\alpha N)^2$, both the resistance and the last term of the average resistivity (15) will diverge when N goes to infinity. In this case, if we successively calculate the respective average with increasing N, the average resistivity will monotonously increase. Consequently, the trend of the successive average resistivity sharply distinguishes the extended states from the localized states and energy gaps. We can use this trend of successive average resistivity as the criterion of the extended state.

In Fig. 8 we plot the logarithmic average resistivity as a function of the size of the Fibonacci chain, where different behavior of the eigenstates is shown. The extended state is characterized by the monotonous decrease of the average resistivity, which monotonously increases for the localized state and neither monotonously decreases nor increases for the intermediate state. Instead, they oscillate. These numerical results confirm again the coexistence of the eigenstates with different localization. Therefore, we may conclude that the term "critical state" is perhaps not accurate enough to describe the properties of electrons in the Fibonacci chain.

The dc resistivity is an important physical quantity for examining the localization. In Fig. 9, the logarithmic resistivity (not average) versus generation is plotted, which corresponds to the extended state $E=0.201\,000$. The oscillation of resistivity with the variation of the system size is characteristic of the quasiperiodicity and finite size effects, which also appears in one-dimensional incommensurate systems.[24] The fact that the logarithmic resistivity decreases with the increase of the generation suggests that this state is extended. For the 40th generation, the number of atoms is remarkably big, $N=102\,334\,155$.

III. EFFECT OF FLUCTUATION

The discussion so far has been restricted to perfect quasicrystals. An interesting question is how the physical properties will be influenced by a deviation from the perfect quasicrystalline symmetry.

In their synchrotron x-ray study of a Fibonacci superlattice, Todd *et al.* have found that for a $\pm 5\%$ fluctuation in layer thickness, the diffraction peaks are neither appreciably smeared out nor reduced in number relative to the predicted ideal pattern. They also carry out a computer simulation and conclude that the intense diffraction peaks are generally affected relatively little by even sub-

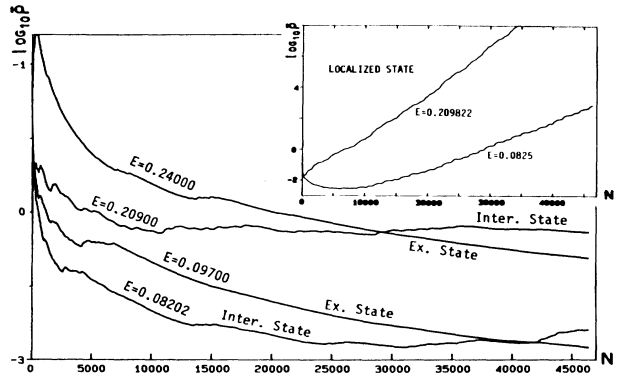

FIG. 8. Average resistivity versus the length N of Fibonacci chain for the on-site model with site energies $E_A=-E_B=0.5$. The localization of the eigenstate is determined by the trend of the average resistivities; localized state monotonously increases, extended state monotonously decreases, and intermediate state neither monotonously decreases, nor monotonously increases.

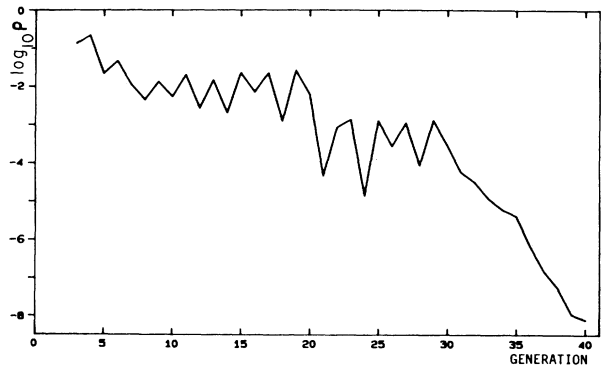

FIG. 9. Logarithmic resistivity versus generation for extended state $E=0.097\,00$ with site energies $E_A=-E_B=0.5$. The 40th generation contains 102 334 155 atoms. The oscillation is characteristic of quasiperiodicity. That the resistivity decreases with the increase of the generation shows that this is an extended state.

stantial amounts of disorder and the diffraction pattern still appears as a dense set of peaks. We are interested in studying, for our simple one-dimensional on-site model of a Fibonacci lattice, that which happens to the electronic spectrum and the localization of eigenstates, when the model is extended to include fluctuations in the site energy.

Two different ways of including random fluctuations in the site energies are considered. In the first case, the random fluctuations are allowed with equal probability for increasing and decreasing the site energy, so the allowed site energies are uniformly distributed over the intervals $(-1-p,-1+p)$ and $(1-p,1+p)$, respectively, where we have chosen the original site energies $E_A=-E_B=1$ and p is the percentage of fluctuation. $p=0$ corresponds to the perfect quasicrystalline order. In the second case, the random fluctuations are restricted to diminishing the difference between E_A and E_B. It means that the fluctuations are only allowed in the intervals $(-1,-1+2p)$ and $(1-2p,1)$, where the range of fluctuations is the same as in the first case, but chosen in a more restricted way. Here $p=0$ also corresponds to the perfect quasiperiodicity, but $p=1$ corresponds to complete disorder in the Anderson sense with uniform distribution of the site energies in the interval $(-1,1)$. The interesting feature with this second approach is that it allows a study of a continuous crossover from perfect quasiperiodicity to complete uniform disorder. The electronic spectra of the second case as a function of p are shown in Fig. 11. As is easily recognized by comparing with Figs. 10 and 11 there is a remarkable difference between the results from the two ways of introducing the random fluctuation. In Fig. 10 there is very little change in the gross features of the spectrum when p increases from 0 to about 0.4 and many of the characteristics of the Fibonacci chain survive even for p up to 1. In the second case the Fibonacci characteristics disappear much faster when p increases and $p=1$ corresponds to a complete structureless spectrum. The reason for this large difference is that in the first case the center of gravity for the site energies stays constant and equal to the value in the original perfect quasicrystal, while in the second case the centers of gravity at $-1+p$ and $1-p$, respectively, both move to zero as p increases to 1. So in the first case the underlying Fibonacci structure still plays a dominant role, while in the second case its influence diminishes as p increases. It is interesting at this point to compare the disappearance of the characteristic Fibonacci energy gaps in Fig. 11 with the decrease of the energy gaps as the site energy amplitude diminishes in Fig. 3. If we were to recall the experiments done by Todd *et al.*,[17] it would be very interesting to see whether an asymmetric fluctuation in the experimental layer thickness also should result in large changes in the diffraction peak pattern.

To examine the influence of the fluctuation to the localization of the eigenstate, in Fig. 12 we plot the logarithmic average resistivity as a function of the size of Fibonacci chain. The chosen eigenenergy $E=0.201\,00$ cor-

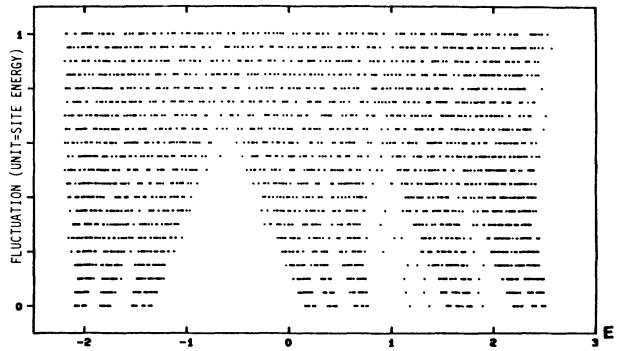

FIG. 11. Same physical situation as in Fig. 10, but the fluctuations of site energy are restricted to diminish the difference between E_A and E_B. The spectra are very sensitive to the increase of the fluctuation. When the fluctuation equals 0.5, the subband structure almost disappears.

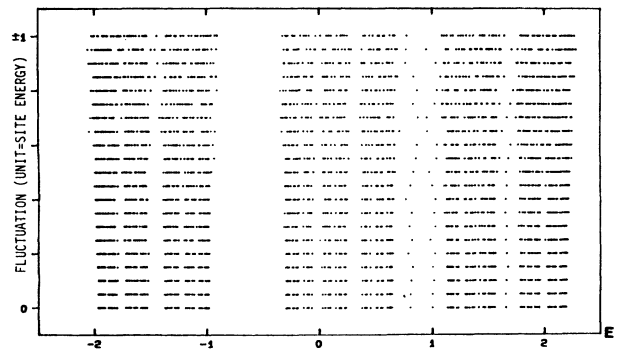

FIG. 10. Phase diagram in the fluctuation versus eigenenergy plane for the 12th generation Fibonacci chain with $E_A=-E_B=1$, $t=-1$. The fluctuations of site energy have equal probability for increasing and decreasing. The gross band structure changes very little if the fluctuations are smaller than ± 0.4.

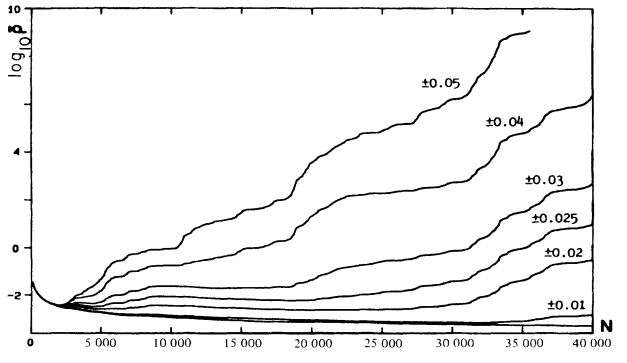

FIG. 12. Logarithmic average resistivity versus system length for different fluctuations. Chosen extended state $E=0.020\,100$ with site energies $E_A=-E_B=0.5$, $t=-1$. When fluctuation equals zero, the graph is a monotonously decreasing curve, which is characteristic of an extended state. With the increase of the fluctuation, the state develops to be more and more localized, which is characterized by the monotonous increase.

responds to an extended state, which is characteristic of the monotonous decrease of the average resistivity. Following the increase of the fluctuation, the average resistivity changes from monotonous decreasing to increasing. It means that the state develops into a localized state. This transition does occur even when the fluctuation is as small as $\pm 1\%$. We can expect that this transition of localization is a general property of a Fibonacci chain, irrespective of the eigenenergy. It is well known that in one-dimensional binary random systems, all the states are localized no matter how weak the disorder is. Therefore this transition induced by the fluctuation, which causes the system to be a disordered one, is not unexpected. On the other hand, Delyon *et al.*[26] have proved that arbitrarily small local perturbations of the potential at two sites make the singular continuous spectrum, which is obtained in some classes of one-dimensional incommensurate systems such as the Aubry model, disappear and instead all eigenstates become exponentially localized. The Fibonacci quasilattices, as an analog of incommensurate systems, also should have the same kind of electronic properties, which is confirmed by our computations.

IV. SUMMARY

We have performed a complete study of the on-site model for a one-dimensional Fibonacci quasicrystal including both the regular and nonperfect cases. The analytic and numerical results show that the on-site model is different from the much more studied transfer model in the global structure of the electronic spectrum, but not in the phonon spectrum. We have established the general relations between the numbers of different constructing elements in the lattice and the numbers of eigenstates in subbands, in which the surface states interestingly play a compensative role for the even generation cases. These relations are confirmed by the spectra obtained and can be easily extended to other one-dimensional quasicrystals.[11]

The question of localization has been addressed with several approaches; the first and second moment, the inverse participation ratio, the spatial distribution of the wave function, the resistivity, and the criterion of successive average resistivity. All these approaches conclude the coexistence of the eigenstates with different localizations, i.e., extended, localized, and intermediate states. At the same time, these states may have some common features which do not appear in the periodic and the disordered systems, such as the self-similarity, quasiperiodicity, and the unusual behavior (decaying and recovering alternately). Therefore, if the term "critical state" is only understood to have the above common features as some authors did then, it does not completely cover the complexity of one-dimensional quasilattices. Therefore, we prefer not to use a single term to describe the electronic properties of quasiperiodic lattices, because in these lattices the localizations are dependent of the parameters and there is not a unique state.

The experiments by Todd *et al.*[17] show the interesting results about the effects of fluctuations in the layer thickness on the x-ray diffraction peak patterns. In Sec. III we show that, to the best of the present authors' knowledge, this is the first time that the influences of the deviations from quasiperiodicity are present on the electronic spectrum. The numerical results show that a symmetric fluctuation of the site energy results in very small changes in the electronic spectra, but that if the fluctuations were nonsymmetric the spectrum would be very sensitively changed. Therefore, the calculations suggest that the x-ray diffraction-peak patterns would be changed if the fluctuations of the layer thickness of the samples were nonsymmetric, because the averaged fluctuations are more important than the amplitude of the fluctuations in question.

It is well known[23] that in the one-dimensional disordered systems all states are localized no matter how weak the disorder is. We can imagine that the quasiperiodic systems also would have the same properties. In Sec. III, using the criterion of successive average resistivity we numerically proved that a very small fluctuation would change the extended state to be localized. This result also agrees with the results for the one-dimensional incommensurate systems.

ACKNOWLEDGMENTS

We would like to thank K. A. Chao for many discussions on the quasiperiodic systems and Zhao-bo Zheng for the EDWW calculation program. We are grateful to M. Kohmoto and M. Fujita for copies of unpublished work. We acknowledge the financial supports from the Swedish Natural Science Research Council; Y. Liu under Grant No. NFR-FFU-3996-127 and R. Riklund under Grant No. NFR-F-HF-1909-102.

*Permanent address: Department of Physics, South China Institute of Technology, Guangzhou, People's Republic of China.

[1]D. S. Schechtman, I. Blech, D. Gratias, and J. W. Cahn, Phys. Rev. Lett. **53**, 1951 (1984).
[2]D. Levine and P. J. Steinhardt, Phys. Rev. B **34**, 596 (1986).
[3]R. Merlin, K. Bajema, R. Clarke, F. Y. Juang, and P. Bhattacharya, Phys. Rev. Lett. **55**, 1768 (1985).
[4]J. E. S. Socolar and P. J. Steinhardt, Phys. Rev. B **34**, 617 (1986).
[5]P. Kramer and R. Neri, Acta Cryst. A **40**, 580 (1984).
[6]V. Elser, Phys. Rev. Lett. **54**, 1730 (1985); Phys. Rev. B **32**, 4892 (1985).
[7]R. K. P. Zia and W. J. Dallas, J. Phys. A **18**, L341 (1985).
[8]M. Kohmoto and J. R. Banavar, Phys. Rev. B **34**, 563 (1986).
[9]M. Kohmoto, Phys. Rev. B **34**, 5043 (1986).
[10]F. Nori and J. P. Rodriguez, Phys. Rev. B **34**, 2207 (1986); Q. Niu and F. Nori, Phys. Rev. Lett. **57**, 2057 (1986).
[11]J. P. Lu, T. Odagaki, and J. L. Birman, Phys. Rev. B **33**, 4809 (1986).
[12]M. Fujita and K. Machita, Solid State Commun. **59**, 61 (1986).
[13]K. Machita and M. Fujita, J. Phys. Soc. (Jpn.) **55**, 1799 (1986).
[14]T. Odagaki and D. Nguyen, Phys. Rev. B **33**, 2184 (1986).

[15]M. Kohmoto, L. P. Kadanoff, and C. Tang, Phys. Rev. Lett. **50**, 1870 (1983).
[16]S. Ostlund, R. Pandit, D. Rand, H. J. Schellnhuber, and E. D. Siggia, Phys. Rev. Lett. **50**, 1873 (1983).
[17]J. Todd, R. Merlin, R. Clarke, K. M. Mohanty, and J. D. Axe, Phys. Rev. Lett. **57**, 1157 (1986).
[18]J. B. Sokoloff, Phys. Rep. **126**, 189 (1985), and references therein.
[19]D. J. Thouless and Q. Niu, J. Phys. A **16**, 1911 (1983).
[20]Youyan Liu (unpublished).
[21]S. Y. Wu and Zhao-bo Zheng, Phys. Rev. B **24**, 4787 (1984); Zhao-bo Zheng, J. Phys. C **19**, L689 (1986).
[22]S. Stafström, R. Riklund, and K. A. Chao, Phys. Rev. B **27**, 6158 (1983).
[23]P. Erdös and R. C. Herndon, Adv. Phys. **31**, 65 (1982).
[24]Youyan Liu, R. Riklund, and K. A. Chao, Phys. Rev. B **32**, 8387 (1985); Youyan Liu and K. A. Chao, *ibid.* **34**, 5247 (1986).
[25]A. Brezini and M. Sebbani, Phys. Status Solidi B **133**, K129 (1986).
[26]F. Delyon, Y. Levy, and B. Soulliard, Phys. Rev. Lett. **54**, 1589 (1985).